

05,13

Dipole-dipole interaction weakening in ensembles of cobalt microspheres with a nonmagnetic core

© S.V. Komogortsev^{1,2,6}, L.A. Chekanova¹, O.V. Shabanova³, A.V. Shabanov¹, I.V. Nemtsev^{1,2,4}, D.S. Neznakhin⁵, E.A. Denisova^{1,2}, V.A. Felk⁶, A.A. Mohov¹, R.S. Iskhakov^{1,6}

¹ Kirensky Institute of Physics, Federal Research Center KSC SB, Russian Academy of Sciences, Krasnoyarsk, Russia

² Siberian Federal University, Krasnoyarsk, Russia

³ Special Designing and Technological Bureau „Nauka“ KSC SB RAS, Krasnoyarsk, Russia

⁴ Krasnoyarsk Scientific Center, Siberian Branch, Russian Academy of Sciences, Krasnoyarsk, Russia

⁵ Ural Federal University after the first President of Russia B.N. Yeltsin, Yekaterinburg, Russia

⁶ Siberian State University of Science and Technology, Krasnoyarsk, Russia

E-mail: komogor@iph.krasn.ru

Received April 29, 2022

Revised April 29, 2022

Accepted May 12, 2022

Magnetic microspheres with nonmagnetic acrylic glass core were fabricated using electroless deposition. There are favorable conditions for magnetic flux closure within each particle. As a result, the dipole-dipole interaction in the powder of such microspheres is reduced drastically. This is the key difference between powders of magnetic microspheres and powders of full magnetic spherical particles witch behavior is significantly affected by the dipole-dipole interaction. The magnetic hysteresis in the cobalt microspheres with nonmagnetic core is significantly large then in the full cobalt particles produced using the same technique.

Keywords: Magnetic microspheres, magnetic dipole-dipole interaction.

DOI: 10.21883/PSS.2022.09.54163.16HH

1. Introduction

Numerous applications of magnetic nano- and microparticles as functional magnetic elements in biomedicine, electronics, catalysis, etc. give rise to a number of problems and requirements for the design of their shape and properties [1–5]. In systems with large arrays of magnetic particles (ferrofluids, ferrogels, magnetic elastomers, granular magnetic composites), the effect of magnetic dipole-dipole interaction is important [6]. Since the dipole-dipole interaction decreases rather slowly with distance ($\propto r^{-3}$), this leads to its non-locality for three-dimensional systems. A correct theoretical account of the influence of such an interaction, especially in ensembles of moving and heterogeneously distributed particles in space, is very difficult [7,8]. Formation of particle clusters under the action of a dipole-dipole interaction affects the properties and is a complex theoretical problem [9]. Also, it has a negative impact on some application characteristics, for example, it reduces the stability of magnetic colloids [10,11]. In this regard, it is important to develop new methods for creating particles that retain high magnetic susceptibility but do not interact, at least in a small external field. The solution in this situation can be the creation of a form

that closes the magnetic flux inside the particle. The ideal shape in this case is a ring, but, firstly, the production of such particles in volumes sufficient for applications has not yet been mastered, and secondly, the anisotropy of the shape of such particles imposes certain restrictions. An interesting solution can be a particle representing a magnetic spherical shell with a cavity or a partially non-magnetic core. In a zero external field with a weak or negative surface magnetic anisotropy constant, the magnetic microstructure of spherical micro- and nanoshells is a magnetization vortex that repeats the contour of a spherical shell and has two cores at diametrically opposite points [12]. The cores of magnetization vortices are topological defects that inevitably arise in closed magnetic shells according to Brouwer's topological fixed point theorem (haired ball theorem) [13]. Thus, the magnetic flux is not completely closed — the magnetic field goes beyond the shell in the region of the vortex cores. The outgoing magnetic flux compared to the total flux within the particle is about l^2/R^2 , where $l = \sqrt{A/4\pi M_s^2}$ (A is exchange constant, M_s is saturation magnetization, R is particle radius (e.g., see [14]). In an experiment, this magnetic flux can be estimated using magnetization jumps [12,15] associated with a jump-like change in the polarity of magnetization vortex cores [12].

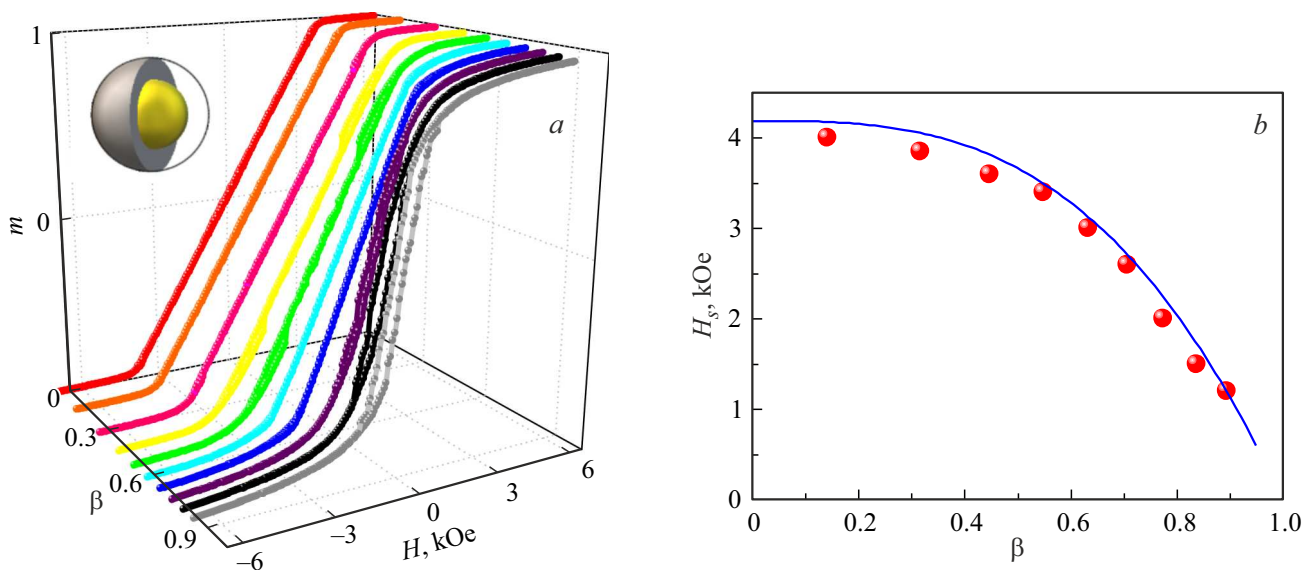


Figure 1. Hysteresis loops for hollow cobalt particles calculated using micromagnetic simulation (left) for particles with different ratios of diameters of the non-magnetic core (D_{in}) and magnetic shell (D_{out}), $\beta = D_{in}/D_{out}$. On the right is the behavior of the H_s field obtained by extrapolating the linear part of the curve to saturation.

For particles with a diameter greater than 100 nm, this jump becomes negligibly small (less than 10^{-3} of M_s). In this article, we report the preparation of spherical magnetic Co particles with a non-magnetic core and the study of their magnetic properties in comparison with the properties of homogeneous spherical particles.

2. Experiment

Particles with a core-shell structure were prepared in two stages. At the first stage, submicron particles of polymethyl methacrylate (PMMA) with a narrow size distribution were synthesized, which were further used as the „core“ base for chemical deposition. The technology for the synthesis of such particles was developed and applied to the synthesis of photonic crystals [16]. Note that these particles can be prepared with a given size from 100 to 300 nm, have a spherical shape and are characterized by high monodispersity. In order to prevent sticking of the particles of polymethyl methacrylate before obtaining a metal coating, metal deposition was carried out on freshly prepared isolated particles in a solution. At the next stage, a metal coating Co(P) was deposited on the surface of the particles by the method of chemical deposition from cobalt salts. The impurity of phosphorus in the particles does not exceed 15 at.%, and the structure is an amorphous solid solution of Co(P) [17]. The magnetization of such a solution (1000 G) is somewhat lower than that for pure cobalt (1400 G), but it is quite high, so below we will call these particles simply cobalt particles. The magnetic hysteresis loops were measured on an MPMS XL-7 EC magnetic measuring complex at a temperature of 300 K.

To analyze the features of magnetic hysteresis in these particles, we performed micromagnetic modeling of magnetic hysteresis loops in core-shell particles using the OOMMF software package [18]. The parameters of the micromagnetic problem were selected corresponding to the experimental parameters of particles or CoP coatings [19–21]. Exchange interaction and magnetic anisotropy constants according [17]: $A = 1 \cdot 10^{-6}$ erg/cm, $K = 4 \cdot 10^5$ erg/cm³, $M_s = 1000$ G. An important feature of these calculations is that the anisotropy constant in this case refers not to the entire particle, but to the crystallites that make up the particle or coating. The sizes of these crystallites are selected equal to 10 nm. The easy magnetization axes of the crystallites are randomly oriented, i.e., the simulation takes into account the heterogeneity inherent in the polycrystalline shell.

3. Micromagnetic modelling

The model hysteresis loops of core-shell particles have different shapes for particles with different shell thicknesses (Fig. 1). The loops are calculated for particles with different values of the parameter $\beta = D_{in}/D_{out}$ — the ratio of the diameter of the nonmagnetic core to the outer diameter of the particle, the shell thickness is related to β as $D_{out}(1 - \beta)/2$. An increase in the shell thickness leads to a decrease in the coercive field (Fig. 1). For a solid spherical particle with a diameter of 250 nm, the coercive field is smaller than the coercive fields of core-shell particles for all calculated cases. The magnetization curve obtained in a numerical experiment (Fig. 1) on one particle near the zero field demonstrates a linear response. So for a solid particle, the saturation field H_s should be

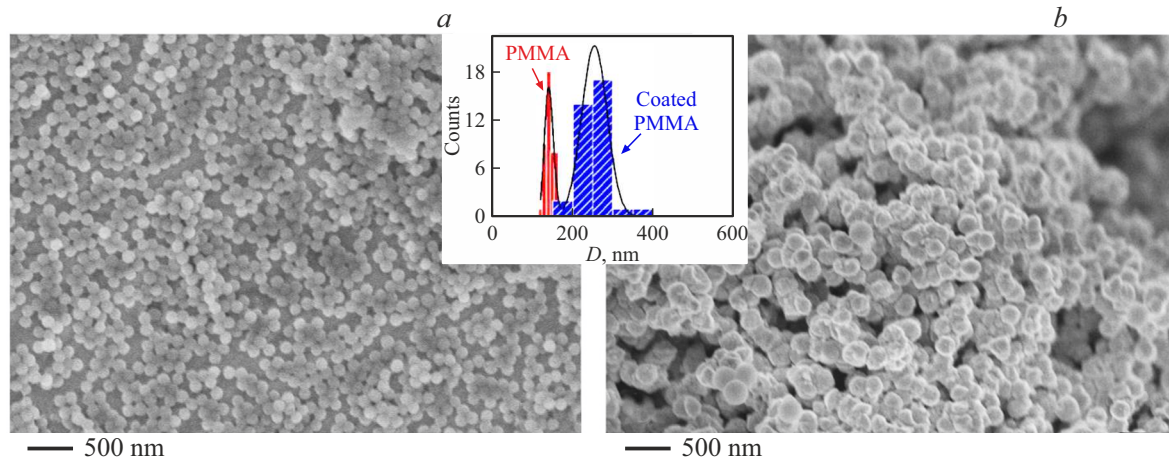


Figure 2. Image of polymethyl methacrylate particles obtained in a scanning electron microscope before (a) and after (b) deposition of Co(P) coating on their surface. The inset shows the size distribution of particles before and after deposition of the Co(P) coating on their surface.

equal to the demagnetizing field $H_s = (4/3)\pi M_s$, while the magnetization grows linearly with the field up to $H = H_s$, i.e., the magnetic susceptibility in the range $(-H_s, H_s)$ is equal to $\chi = M_s/H_s$, which is observed in Fig. 1 at $\beta = 0$. The magnetization curves of magnetic shells demonstrate a sharper linear increase in magnetization with the field than for solid particles, in the region of low fields, with the thinning of the magnetic shell. The range of the linear section implementation in the shells is limited by fields lower than H_s , above which magnetization proceeds non-linearly, and the magnetization distribution resembles the structure of an onion, the axis of which coincides with the field direction. The description of the linear section in low fields as $M = H/H_s$ enables to estimate the value of H_s for particles with different shell thicknesses (Fig. 1). It can be seen in Fig. 1, b that this field agrees well with the estimate $H_s = (4/3)\pi M_s \nu = (4/3)\pi M_s (1 - \beta^3)$, where ν is volume fraction of the magnetic shell [22,23].

4. Morphology and particle sizes

The images obtained with the FE-SEM S-5500 scanning electron microscope (Hitachi, Japan) show that the diameter of PMMA particles after cobalt coating deposition on their surface increased, despite the fact that their spherical shape generally preserved (Fig. 2). It is also seen in Fig. 2 that, if the Plexiglas particles were characterized by a high degree of monodispersity before deposition, then after deposition not only the particle diameter increased, but also the size dispersion increased. Before deposition, the particles are lognormally distributed. After deposition, the size distribution is better described by a Gaussian function. The average particle sizes $D_{before} = (141 \pm 3)$ nm before deposition and $D_{after} = (253 \pm 3)$ nm after deposition allow us to estimate the shell thickness as $t = \frac{(D_{after} - D_{before})}{2} = (56 \pm 5)$ nm.

The D_{after} distribution width is 32 nm. Thus, the thickness of the shell in different particles varies from 40 to 72 nm.

5. Magnetic properties of particles

The hysteresis loop of core-shell particles is much wider than that of conventional Co(P) powders of a given size (Fig. 3). In articles [17,19,24] it is shown that the structure of Co(P) particles obtained by chemical deposition is a heterophase mixture of metastable Co(P) solid solutions with an amorphous structure, FCC and HCP. The magnetic properties of these phases are significantly different; therefore, the properties of particles change following the changes in the phase composition depending on the particle size and phosphorus concentration [17]. In this case we are dealing with particles and coatings of Co(P) containing 15 at.% P. The main phase of cobalt particles with such a phosphorus content is an amorphous solid solution [17]. The coercive force of solid particles $\text{Co}_{85}\text{P}_{15}$ changes in size from 0.1 to $3\mu\text{m}$ in the range from 100 to 200 Oe [19]. Fig. 3 shows the magnetization curve measured on a powder of solid particles with a particle size of 300 nm close to the outer diameter of the studied particles with a nonmagnetic core. The hysteresis loop of Co(P) particles with a nonmagnetic core is characterized by a much stronger hysteresis (Fig. 3). The coercive force here is 700 Oe (Fig. 3).

6. Discussion

Both in experiment and in micromagnetic simulation, the coercive field of a solid particle turns out to be smaller than for a particle with a core-shell structure (Fig. 3). However, in the experiment, saturation of solid particles is achieved in lower fields. In the simulation, this situation is inverted. In addition, for „nonmagnetic core-magnetic shell“ particles we obtain a remarkable agreement between

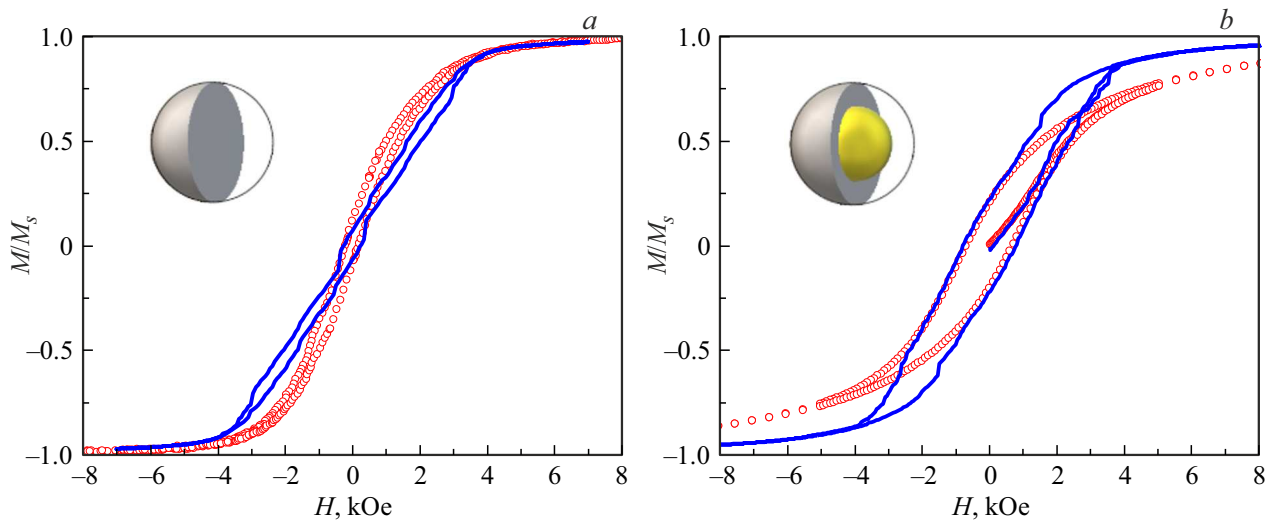


Figure 3. Hysteresis loops of solid particles (a) and particles of Co@PMMA (b). Experimental data are round symbols, solid line is data obtained by numerical simulation.

the numerical and experimental magnetization curves in low fields. Namely, here it is possible to achieve agreement both on the slope of the magnetization curve near the zero field and on the magnitude of the coercive force.

Let's discuss the reasons leading to coincidences and differences between experimental and numerical data. The magnetization curve calculated using micromagnetic simulation refers to a single particle. Comparison of the results of such simulation with the experimental results measured on the powder implies the possibility of neglecting the effects of the dipole-dipole interaction in the system of particles. To estimate the effect of this interaction on the hysteresis loop, it is important to estimate the parameter $\kappa = 4K/M_s^2$ [25]. Using the crystallite anisotropy constant $K = 4 \cdot 10^5$ erg/cm³ and $M_s = 1000$ G we obtain $\kappa = 16$. If the constant K corresponded not to a crystallite, but to a particle, this would mean that the effect of the dipole-dipole interaction is insignificant. The correct selection of the particle anisotropy constant for such an assessment is an important and difficult problem. The point is that the crystallite magnetic anisotropy constant, which we use in the simulation, can significantly exceed the magnetic anisotropy constant of a particle containing many crystallites. In article [26] this is demonstrated for single-domain particles. In addition, sufficiently large particles (more than 30 nm), consisting of crystallites with randomly oriented easy magnetization axes, contain more than one magnetic domain, dividing into so-called stochastic magnetic domains [21,27]. The studied particles are characterized by the presence of random magnetic anisotropy and are large enough to use the earlier estimate of their anisotropy constant for stochastic domains in Co₈₅P₁₅ alloys. According to [27] this constant is $\sim 8 \cdot 10^3$ erg/cm³ and now the estimate is $\kappa = 0.3$. Thus, in the system of Co(P) particles, the influence of the dipole-dipole interaction can be significant.

The closure of the magnetic flux inside a particle with a nonmagnetic core should lead to a sharp decrease in the dipole-dipole interaction in the system of particles. This closure is the more effective, the smaller the external field. In solid magnetic micro- and nanoparticles, magnetic flux closure either does not occur at all (single-domain particles) or is much less efficient than in hollow particles. In the case of effective flux closure, the dipole-dipole interaction between particles is negligibly small. Indeed, it is for core-shell particles that a remarkable agreement is observed between the model and experimental loops near the zero field, while for solid particles we see a significant difference in the behavior of the experimental and model hysteresis loops. As Fig. 1 shows, the slope of the linear part of the magnetization curve is sensitive to the thickness of the magnetic shell. Note that the numerical curve in Fig. 3, b demonstrating the same slope as the experimental loop in the region of low fields, was obtained for a particle with dimensions (shell thickness 50 and core diameter 140 nm) close to those that are estimated by microscopic images. This coincidence is an additional argument both in favor of the reliability of particle size characterization and the results of micromagnetic calculations.

The fact that the dipole interaction is weakened in an ensemble of hollow cobalt particles is also evidenced by the good agreement between the calculated and experimental coercive forces (Fig. 3, b). To interpret the coercive force of particles with a polycrystalline structure, the dimension in the system of exchange-coupled crystallites becomes important [28–30]. Increasing the thickness of the shell, which contains more than one crystallite across, effectively increases the dimension of the system, which should lead to a decrease in the coercive force [28,31]. It is this behavior that we observe in Fig. 3, b.

The neglect of the dipole-dipole interaction, which is justified for small fields (on the order of or less than

the coercive field), becomes incorrect for sufficiently large fields, where the particles are magnetized almost uniformly. In this case, each particle is the source of the magnetic field generated by the magnetic dipole moment of the particle. With this we attribute the difference in saturation fields for core-shell particles and solid spheres in simulation and in experiment. Thus, the experimental magnetization curves demonstrate saturation in lower fields for solid particles, while the numerical results, on the contrary, in a core-shell particle (Fig. 3). The experimental result can be explained by the formation of chains and clusters, which are oriented in a sufficiently large field and, thereby, increase magnetic susceptibility [7,32]. This effect should be more pronounced for particles with a large magnetic moment and a more uniform distribution of magnetization. Solid particles of cobalt satisfy these conditions better than magnetic shells of cobalt.

7. Conclusion

In conclusion, we list important results.

1. Magnetic microspheres with a non-magnetic acrylic glass core can be prepared by chemical deposition.

2. In the region of low magnetic fields, the magnetic flux closes within the shell of one particle with a nonmagnetic core, which is reflected in the coincidence of the experimental magnetization curve measured on the powder and the results of micromagnetic calculations performed for a single spherical particle with a nonmagnetic core.

3. The magnetic hysteresis of cobalt microspheres with a nonmagnetic core is significantly increased in comparison with solid cobalt particles due to the anisomerism of the magnetization correlation volumes.

Acknowledgments

The authors thank the Krasnoyarsk Regional Center of Research Equipment of Federal Research Center „Krasnoyarsk Science Center SB RAS“ for the provided equipment.

Funding

The study was done with financial support from the Russian Foundation for Basic Research, Government of Krasnoyarsk Territory and the Krasnoyarsk Regional Fund of Science within scientific project No. 20-42-240001.

Conflict of interest

The authors declare that they have no conflict of interest.

References

- [1] D. Sander, S.O. Valenzuela, D. Makarov, C.H. Marrows, E.E. Fullerton, P. Fischer, J. McCord, P. Vavassori, S. Mangin, P. Pirro, B. Hillebrands, A.D. Kent, T. Jungwirth, O. Gutfleisch, C.G. Kim, A. Berger. *J. Phys. D* **50**, 363001 (2017). doi: 10.1088/1361-6463/aa81a1.
- [2] R.L. Stamps, S. Breitreutz, J. Åkerman, A.V. Chumak, Y. Otani, G.E.W. Bauer, J.-U. Thiele, M. Bowen, S.A. Maletich, M. Kläui, I.L. Prejbeanu, B. Dieny, N.M. Dempsey, B. Hillebrands. *J. Phys. D* **47**, 333001 (2014). doi: 10.1088/0022-3727/47/33/333001.
- [3] A. Fernández-Pacheco, R. Streubel, O. Fruchart, R. Hertel, P. Fischer, R.P. Cowburn. *Nature Commun.* **8**, 15756 (2017). doi: 10.1038/ncomms15756.
- [4] S. Kantorovich, E. Pyanzina, F. Sciortino. *Soft Matter* **9**, 6594 (2013). doi: 10.1039/c3sm50197c.
- [5] J.G. Donaldson, P. Linse, S.S. Kantorovich. *Nanoscale* **9**, 6448 (2017). doi: 10.1039/C7NR01245D.
- [6] M. Hod, A. Dobroserdova, S. Samin, C. Dobbrow, A.M. Schmidt, M. Gottlieb, S. Kantorovich. *J. Chem. Phys.* **147**, 084901 (2017). doi: 10.1063/1.4995428.
- [7] A.O. Ivanov, S.S. Kantorovich, V.S. Zverev, A.V. Lebedev, A.F. Pshenichnikov, P.J. Camp. *J. Magn. Magn. Mater.* **459**, 252 (2018). doi: 10.1016/j.jmmm.2017.10.089.
- [8] A.O. Ivanov, V.S. Zverev, S.S. Kantorovich. *Soft Matter* **12**, 3507 (2016). doi: 10.1039/C5SM02679B.
- [9] A.O. Ivanov, S.S. Kantorovich, E.N. Reznikov, C. Holm, A.F. Pshenichnikov, A.V. Lebedev, A. Chremos, P.J. Camp. *Phys. Rev. E* **75**, 061405 (2007). doi: 10.1103/PhysRevE.75.061405.
- [10] B. Sanz, M.P. Calatayud, N. Cassinelli, M.R. Ibarra, G.F. Goya. *Eur. J. Inorg. Chem.* **2015**, 4524 (2015). doi: 10.1002/ejic.201500303.
- [11] F. Arteaga-Cardona, K. Rojas-Rojas, R. Costo, M.A. Mendez-Rojas, A. Hernando, P. de la Presa. *J. Alloys Compd.* **663**, 636 (2016). doi: 10.1016/j.jallcom.2015.10.285.
- [12] M.I. Sloika, D.D. Sheka, V.P. Kravchuk, O.V. Pylypovskiy, Y. Gaididei. *J. Magn. Magn. Mater.* **443**, 404 (2017). doi: 10.1016/j.jmmm.2017.07.036.
- [13] M. Eisenberg, R. Guy. *Am. Math. Mon.* **86**, 571 (1979). doi: 10.1080/00029890.1979.11994857.
- [14] V.P. Kravchuk, D.D. Sheka. *FTT* **49**, 1834 (2007) (in Russian). <http://journals.ioffe.ru/articles/viewPDF/3192>.
- [15] V.P. Kravchuk, U.K. Rößler, O.M. Volkov, D.D. Sheka, J. van den Brink, D. Makarov, H. Fuchs, H. Fangohr, Y. Gaididei. *Phys. Rev. B* **94**, 144402 (2016). doi: 10.1103/PhysRevB.94.144402.
- [16] A.V. Shabanov, O.V. Shabanova, M.A. Korshunov. *Colloid J.* **76**, 113 (2014). doi: 10.1134/S1061933X14010128.
- [17] L.A. Chekanova, E.A. Denisova, O.A. Goncharova, S.V. Komogortsev, R.S. Iskhakov. *Fizika metallov i metalovedenie*, **114**, 136 (2013) (in Russian). doi: 10.7868/S0015323013020046.
- [18] M.J. Donahue, D.G. Porter. *OOMMF user's guide*, version 1.0, Gaithersburg, MD, (1999). doi: 10.6028/NISTIR.6376.
- [19] L.A. Chekanova, E.A. Denisova, R.S. Iskhakov. *IEEE Trans. Magn.* **33**, 3730 (1997). doi: 10.1109/20.619553.
- [20] V.A. Ignatchenko, R.S. Iskhakov, G.V. Popov. *ZhETF* **82**, 1518 (1982) (in Russian).
- [21] R.S. Iskhakov, V.A. Ignatchenko, S.V. Komogortsev, A.D. Bayayev. *Pis'ma v ZhETF* **78**, 1142 (2003) (in Russian).
- [22] M. Beleggia, D. Vokoun, M. De Graef. *J. Magn. Magn. Mater.* **321**, 1306 (2009). doi: 10.1016/j.jmmm.2008.11.046.
- [23] B. Nam, J. Kim, K. Ki Hyeon. *J. Appl. Phys.* **111**, 07E347 (2012). doi: 10.1063/1.3679579.
- [24] R.S. Iskhakov, L.A. Chekanova, E.A. Denisova. *Phys. Solid State* **41**, 416 (1999). doi: 10.1134/1.1130794.

- [25] S.V. Komogortsev, V.A. Fel'k, O.A. Li. *J. Magn. Magn. Mater.* **473**, 410 (2019). doi: 10.1016/j.jmmm.2018.10.091.
- [26] N.A. Usov, A. Zhukov, J. Gonzalez. *J. Non. Cryst. Solids* **353**, 796 (2007). doi: 10.1016/j.jnoncrysol.2006.12.043.
- [27] R.S. Iskhakov, S.V. Komogortsev. *Phys. Met. Metallogr.* **112**, 666 (2011). doi: 10.1134/S0031918X11070064.
- [28] R.S. Iskhakov, S.V. Komogortsev, A.D. Balayev, A.V. Okotrub, A.G. Kudashov, V.L. Kuznetsov, Yu.V. Butenko. *Pis'ma v ZhETF* **78**, 271 (2003) (in Russian).
- [29] S.V. Komogortsev, V.A. Felk, R.S. Iskhakov, G.V. Shadrina. *ZhETF* **152**, 379 (2017) (in Russian). doi: 10.7868/S0044451017080144.
- [30] S.V. Komogortsev, R.S. Iskhakov, V.A. Felk. *ZhETF* **155**, 886 (2019) (in Russian). doi: 10.1134/S0044451019050122.
- [31] R.S. Ishakov, S.V. Komogortsev, A.D. Balaev, L.A. Chekanova. *Pis'ma v ZhETF* **72**, 440 (2000) (in Russian).
- [32] A.O. Ivanov, S.S. Kantorovich, E.A. Elfimova, V.S. Zverev, J.O. Sindt, P.J. Camp. *J. Magn. Magn. Mater.* **431**, 141 (2017). doi: 10.1016/j.jmmm.2016.09.119.